# Highly efficient nitrogen fixation enabled by an atmospheric pressure rotating gliding arc

Hang Chen[1], Angjian Wu*[1], Stéphanie Mathieu[3], Peihan Gao[3], Xiaodong Li[1], Bo Z. Xu[4], Jianhua Yan[1], Xin Tu[2*]

[1] State Key Laboratory of Clean Energy Utilization, College of Energy Engineering, Zhejiang University, Hangzhou, 310027, P. R. China

[2] Department of Electrical Engineering and Electronics, University of Liverpool, Liverpool L69 3GJ, UK

[3] School of Electrical and Computer Engineering, Cornell University, Ithaca, New York, NY 14853, USA

[4] School of Civil and Environmental Engineering, Washington State University, Pullman, Washington, WA 99164, USA

***Corresponding authors**

Angjian Wu, State Key Laboratory of Clean Energy Utilization, Zhejiang University, 310027 Hangzhou, China.

Email: wuaj@zju.edu.cn

Xin Tu, Department of Electrical Engineering and Electronics, University of Liverpool, L69 3GJ Liverpool, United Kingdom.

Email: xin.tu@liverpool.ac.uk

**Abstract:**

A rotating gliding arc is proposed as a promising alternative to enable direct nitrogen fixation from ubiquitous air under mild conditions. The effect of different process parameters on $NO_x$ generation and energy consumption has been investigated through a combination of experiments and artificial neural network modeling. The optical emission spectroscopic diagnostics together with electrical diagnostics and high-speed photography has been used to understand the variation of the discharge characteristics. The lowest energy consumption of $NO_x$ production (4.2 MJ/mol) is achieved at a gas flow rate of 12 L/min and an $O_2$ concentration of 20 vol.%. The simulation results from the ANN model show a good agreement with the experimental data and the model enables us to evaluate the relative importance of the process parameters to the reaction performance.

**Keywords:** Non-thermal plasma; Rotating gliding arc; Nitrogen fixation; $NO_x$ synthesis; Artificial neural network; Machine learning

## 1. Introduction

Nitrogen fixation, usually defined as the conversion of nitrogen molecules ($N_2$) into nitrogen compounds (such as ammonia, nitric oxides or nitrate) through redox reactions, plays a significant role in the nitrogen cycle and industrial agriculture. To date, the Haber-Bosch process (HBP) is undisputedly the dominant and successful artificial nitrogen fixation technology since its first introduction in 1913, contributing to nearly 90% of global $NH_3$-based fertilizer [1, 2]. However, intensive energy inputs and harsh operating conditions (450-600 $^oC$, 150-350 atm) are prerequisites for the HBP owing to the high stable triple bond of the nitrogen molecule (N≡N, 948 kJ/mol). It has been reported that the HBP consumes 1~2% of the world's energy and emits more than 300 million metric tons of $CO_2$ annually [3, 4]. Therefore, it is imperative to develop eco-friendly and energy-efficient technologies to achieve green nitrogen fixation.

Alongside other alternatives to the HBP, such as electrocatalysis, photocatalysis, thermal catalysis, non-thermal plasma (NTP) attracts considerable interest for nitrogen fixation because of its advantages of high chemical reactivity, parameter-tuning flexibility and mild operating conditions [2, 5-11]. Actually, the Birkeland-Eyde process based on thermal plasma $NO_x$ synthesis was the first commercial attempt of nitrogen fixation prior to HBP. However, the thermal-equilibrium nature of the plasma and the frequent occurrence of electric shortage at that time limited its further development [12]. Contrary to thermal plasma, NTP is highly non-equilibrium, which means that the majority of the energy injected into the NTP is used to generate energetic electrons and chemically reactive species (e.g., radicals, excited molecules, ions and

atoms), rather than to heat the background gas [13, 14]. As a result, NTP has great potential to achieve a theoretical limit of power consumption of ~0.2 MJ/mol of $N_2$, which is about 2.5 times lower than that of HBP (~0.48 MJ/mol of $N_2$) [15]. Moreover, NTP offers the flexibility to be easily integrated with renewable energy sources (e.g. solar, wind and wave power) with the merits of quick startup and shutdown. As the booming development of renewable energy will lead to a projected 30% cost reduction in renewable electricity by 2050 [16], NTP technologies have great potential to be economically competitive for fertilizer production and energy storage.

In this context, increasing research efforts have been devoted to investigating non-thermal plasma synthesis of $NO_x$ (a mixture of NO and $NO_2$) for nitrogen fixation. Patil et al. developed a knife-shaped pulsed gliding arc (GA) plasma reactor for $NO_x$ synthesis, achieving 4000 ppm $NO_x$ at a flow rate of ~1 L/min [11]. Graves et al. compared different plasma systems (e.g. glow discharge, spark discharge and propeller arc) for nitrogen fixation via air oxidation [17, 18]. Yang et al. investigated nitrogen fixation at the interface in air/water system using an air GA, with a maximal $NO_x$ production rate of 5.5 mg/L at an air flow rate of 3.2 L/min [19]. However, this promising nitrogen fixation process involves complex multi-step physical and chemical processes and still face challenges such as low $NO_x$ yield, low treatment capacity and high energy consumption. A better understanding of the roles of different process parameters is essential to optimize the performance of nitrogen fixation using NTP. Most of previous experimental works on plasma $NO_x$ production were investigated using standard approaches, which examines the influence of only one of the process

parameters in isolation from the others each time. It is also time consuming and labor intensive to screen a large number of process parameters to get a full picture of the plasma process using this conventional method. The quantified relative importance of different process parameters and the interactive effects of different process parameters on the performance of the plasma $NO_x$ production process is largely unclear. Plasma chemical kinetic modeling provides a promising alternative for the prediction and optimization of plasma chemical processes. For instance, Wang et al. developed a 0D plasma chemical model to describe the $N_2/O_2$ reaction in a GA discharge, which involved 48 species and hundreds of reactions [20]. Nevertheless, the elaboration of a comprehensive model of NTP is very time-consuming and thus it may not be the best option for a fast and cost-effective prediction and optimization of highly complex non-linear plasma systems. To tackle this issue, artificial neural networks (ANNs) have been recognized as a promising solution for regression analysis. Owing to their advantages of self-adaption, self-configuration and self-learning, ANNs can build a mapping of the input and output variables based on a limited amount of experimental data with sufficient process units (neurons). Thereby, a well-trained and developed ANN model could forecast the interaction between the input process parameters and the output reaction performance of the nitrogen fixation process with good accuracy. In addition, the model enables us to better understand the quantified relative importance of different process parameters in the plasma $NO_x$ production process. However, using ANNs for plasma chemical processes is still limited, especially for plasma-driven nitrogen fixation [21-23].

In this work, a rotating gliding arc (RGA) discharge reactor has been developed for the production of $NO_x$ (NO and $NO_2$) from $N_2/O_2$ mixtures. The influence of $O_2$ concentration, gas flow rate, and applied voltage on the performance of $N_2$ oxidation ($NO_x$ concentration and energy consumption) and the relative importance of different process parameters, are evaluated through a combination of experiments and ANN modeling. The electrical characteristics and arc dynamics of the RGA discharge are investigated to provide an intuitive illustration of the nitrogen fixation process under different operating conditions. Furthermore, optical emission spectroscopic (OES) diagnostics has been used to study the formation of reactive species and the possible reaction mechanisms involved.

## 2. Materials and Methods

### *2.1 Experimental setup*

Figure 1 shows the experimental setup for the $NO_x$ synthesis. The RGA reactor is made of stainless steel, with a cone-shaped anode inside (base diameter of 36 mm and the height of 55 mm) and an external cylindrical cathode. The narrowest gap between the two electrodes is 3 mm. Magnetic rings are placed outside the RGA reactor to form a vertical magnetic field. A cyclone unit is designed to form a swirling gas flow inside the reactor to enhance the interaction between the arc and the reactants. Herein, $O_2$ (99.99%)/$N_2$ (99.99%) mixtures and air are selected as the reactants. The total flow rate is controlled by a mass flow controller (MFC) and adjusted between 4 L/min and 12 L/min, with an $O_2$ concentration set in the range of 10 vol.% to 60 vol.%. The RGA

reactor is connected to a direct current (DC) power supply (Teslaman TLP 2040, 10 kV). A resistance (40 kΩ) is connected in series with the reactor to limit the arc current. The electrical signals are sampled using a digital oscilloscope (Tektronix DPO4034B), while the dynamic characteristics of the RGA discharge are recorded using a high-speed camera (Phantom V2512) with a sampling rate of 39000 frames per second (fps). The gas products are diluted with nitrogen (99.9%) and pumped into a gas analyzer (MGA-5) for the quantification of $NO_x$ (NO and $NO_2$) concentration. All the measurements are repeated 3 times. The $N_2O$ concentration is below the detection limit of the gas analyzer and is thus not considered. Previous works also reported that the formation of $N_2O$ in GA was very low even though the greenhouse gas impact of $N_2O$ is significant [11]. The emission spectra of the RGA discharge is recorded using a Princeton monochromator (Princeton SP 2750) equipped with an intensified charge-coupled device (ICCD, Princeton PIX-100B).

The specific energy input (SEI) is defined as follows.

$$\text{SEI}\left(\frac{\text{kJ}}{\text{L}}\right) = \frac{\text{U}\times\text{I}(\frac{J}{s})\times 10^{-3}(\frac{\text{kJ}}{J})\times 60(\frac{s}{min})}{\text{Flow rate}\ (\frac{L}{min})} \quad (1)$$

where U (V) is the average arc voltage and I (A) is the average arc current.

The energy consumption of $NO_x$ production is calculated as follows.

$$\text{Energy consumption}\ (\frac{\text{MJ}}{mole}) = \frac{\text{SEI}(\frac{\text{kJ}}{\text{L}})\times 10^{-3}(\frac{\text{MJ}}{kJ})}{\text{NO}_\text{X}\ \text{produced}\ (\frac{mole}{L})} \quad (2)$$

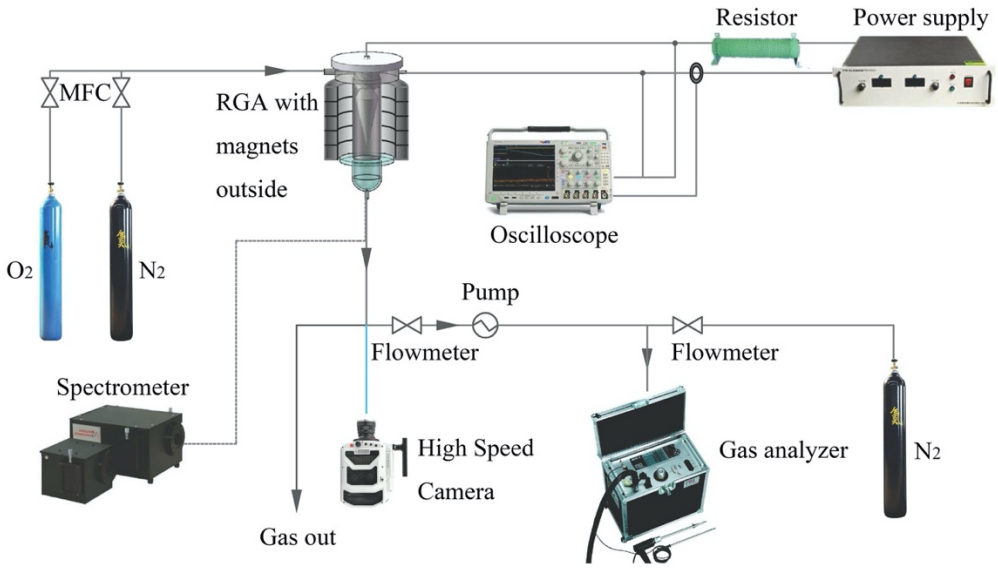


**Figure 1. Experimental scheme of RGA system used for nitrogen fixation**

### *2.2 Artificial neural network*

ANN consists of highly interconnected neurons to process information by their dynamic state response to inputs. A typical ANN model includes an input layer, an output layer and one or more hidden layers, while each layer consists of several neurons and communication paths [24]. Back-propagation (BP) is a widely used supervised learning algorithm for training the multilayer ANN, by providing the desired relationship between input and output data based on the minimization of an error between simulated and experimental data.

Herein, a three-layer BP ANN model (input, hidden and output layer) is developed to simulate and predict plasma synthesis of $NO_x$. Three key process parameters including gas flow rate, applied voltage and $O_2$ concentration are used as the input variables for the input layer, while the output layer consists of two critical performance indicators ($NO_x$ concentration and energy consumption), as illustrated in Figure 2. The experimental data are randomly divided into training and test sets. The Root Mean

Square Prop (RMSprop) training algorithm with a Rectified Linear Unit (ReLU) activation function is used to train the ANN model. To reduce the overfitting of the model, the trick of L2 regularization is employed. Based on the optimization of the connection weights between different layers, the optimal neuron number at the hidden layer is determined to be 32 with a minimum mean square error (MSE). Herein, the MSE on the training set and test set is 0.025 and 0.034, respectively. The optimal ANN model is obtained with a correlation coefficient of 0.912, indicating a good agreement between simulated and experimental data. For comparison, the experimental data are also trained using another 6 linear or non-linear regression methods (Table.S1), including support vector machines (SVM) with 3 different kernels, random forests, k-nearest neighbor regression and ridge regression. As a result, the ANN model shows the best performance as confirmed by the least MSE value on the testing set. For non-linear regression problems, conventional machine learning (ML) methods are restricted by their given mathematical structures and limited flexibility. In other words, an inappropriate mathematical structure or data mapping method decreases the performance of the ML model. Therefore, we choose the ANN model for the optimization and prediction of the plasma $NO_x$ production using the RGA.

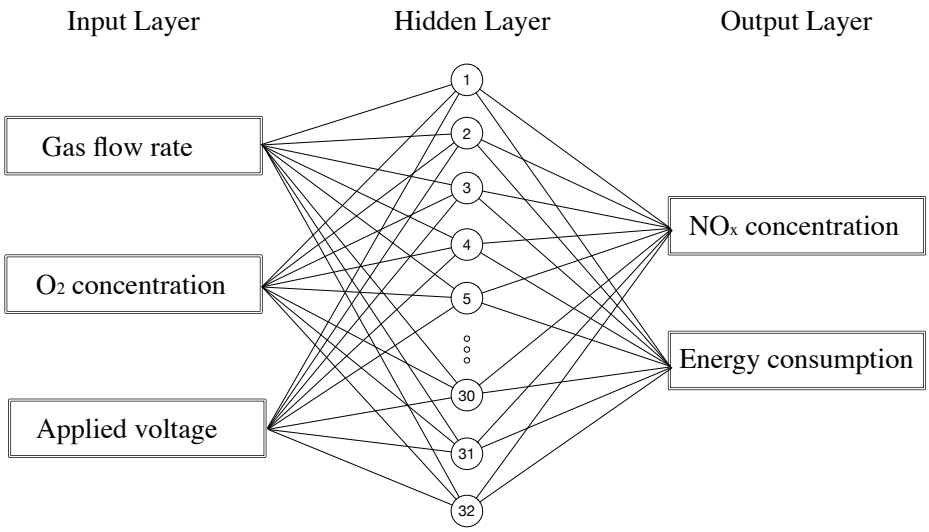


**Figure 2. Optimized three-layer ANN model**

The relative importance of each process parameter is determined by calculating the average absolute gradient of the ANN model using a Monte Carlo simulation. Firstly, a million normalized random inputs are imported into the ANN model. Then, the corresponding gradient of the ANN model for every generated input is calculated using the BP algorithm:

$$\frac{\partial F}{\partial X_i} = \sum_j^{N_h} \left( \frac{\partial f_{1j}}{\partial X_i} \times \frac{\partial h_j}{\partial f_{1j}} \times \frac{\partial f_2}{\partial h_j} \times \frac{\partial F}{\partial f_2} \right) \quad (3)$$

where F stands for the ANN model; $X_i$ refers to the $i_{th}$ input neuron; $N_h$ is the number of hidden neurons; $f_{1j}$ is the linear mapping between the input layer and $j_{th}$ hidden neuron; $f_2$ is the linear mapping between the hidden layer and the target output neuron; $h_j$ refers to the $j_{th}$ hidden neuron. Finally, the absolute gradients are aggregated and averaged to determine the relative importance of a process parameter:

$$I_i = \frac{g_i}{\sum_j^n g_j} \quad (4)$$

$$g_i = \frac{\sum_j^{N_m} \left| \frac{\partial f}{\partial X_{ij}} \right|}{N_m} \quad (5)$$

where $I_i$ is the relative importance; $g_i$ stands for the gradient component for the $i_{th}$ input; $X_{ij}$ refers to the $i_{th}$ input component of the $j_{th}$ randomly generated by the ANN; $N_m$ is the number of randomly generated ANN inputs.

## 3. Result and discussion

### *3.1 Effect of gas flow rate*

The gas flow rate has a considerable impact on the plasma reaction performance in terms of $NO_x$ concentration and energy consumption (Figure 3(a) and (b)). Clearly, the concentration of $NO_x$ decreases with the increase of the gas flow rate, regardless of the $O_2$ concentration (Figure 3(a)). Increasing the gas flow rate decreases the residence time of the gas in the plasma zone, which reduces the interactions between the feeding gas and the arc discharge. On the other hand, increasing the gas flow rate from 4 L/min to 12 L/min decreases the SEI from 4.5 kJ/L to 1.6 kJ/L, suggesting that less input energy per unit volume of the reactant gas. Both of these effects negatively affect the production of $NO_x$ in this process. By contrast, we find that the variation of the gas flow rate significantly changes in the arc properties.

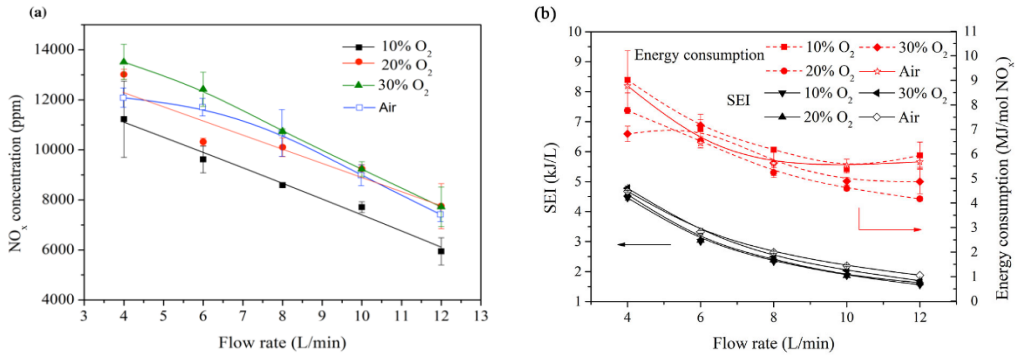


**Figure 3. The effect of gas flow rate on (a) $NO_x$ concentration; (b) SEI and energy consumption at an applied voltage of 10 kV.**

As shown in Figure 4, increasing the gas flow rate lengthens the arc, thus increases the non-equilibrium degree and the reaction zone in the RGA reactor [25], which can

facilitate the formation of more energetic electrons and reactive species in the plasma, consequently enhancing the activation of $N_2$ and the subsequent formation of $NO_x$. However, compared to the opposite and negative effects, this positive effect induced by the increased arc length is less important in the plasma synthesis of $NO_x$

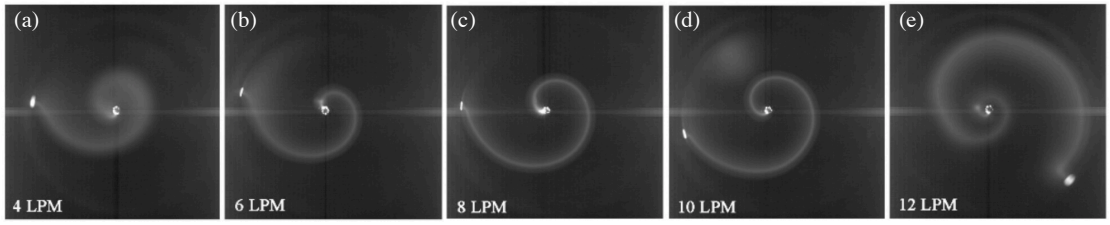


**Figure 4. The effect of gas flow rate on the arc length ($O_2$ concentration of 20 vol.%, applied voltage of 10 kV)**

Figure 3 (b) shows that the variation in energy consumption as a function of the gas flow rate follows the same trend as $NO_x$ concentration. The energy consumption is decreased by about 35% when increasing the gas flow rate from 4 to 12 L/min. The lowest energy consumption of $NO_x$ (~4.2 MJ/mol) is obtained at the highest gas flow rate of 12 L/min and an $O_2$ concentration of 20 vol.%. Increasing the gas flow rate shows a more significant effect on the decrease of the SEI instead of the $NO_x$ concentration, leading to lower energy consumption at a higher flow rate. When using air extracted directly from the surrounding environment as the nitrogen source, the $NO_x$ concentration and energy consumption are within the range measured when using $O_2$ is used at a concentration varying from 10 vol.% to 30 vol.% (Figure 3 (a) and (b)).

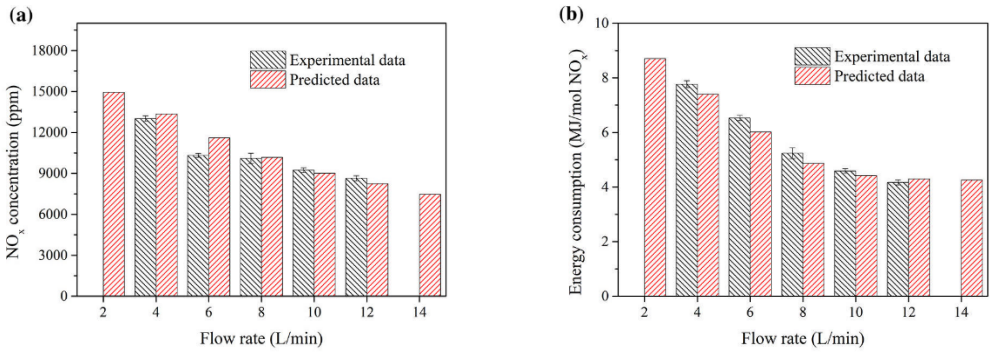


**Figure 5. Comparison of experimental and predicted data in terms of (a) $NO_x$ concentration; (b) energy consumption ($O_2$ concentration of 20 vol.% and applied voltage of 10 kV)**

Figure 5 (a) and (b) illustrate that the predicted values from the ANN model show a fairly good agreement with the experimental results when changing the flow rate at an $O_2$ concentration of 20 vol.%. Furthermore, the ANN model enables us to predict the performance of plasma $NO_x$ production under other conditions not experimentally tested (e.g., 2.5 L/min and 13.5 L/min). The results show that a lower gas flow rate (< 10 L/min) leads to higher $NO_x$ concentration at the expense of increased energy consumption, while further increasing the gas flow rate has a limited impact on the energy consumption.

Previous works reported that the limitations of using plasma for the production of nitrogen oxides are mainly reflected through the low $NO_x$ concentration and limited treatment capacity [11, 18, 26-28]. For example, using a knife-shaped GA reactor, Patil et al. reported a $NO_x$ concentration of 14000 ppm, but this was achieved at the expense of a very low gas flow rate (0.5 L/min) and high energy consumption (7.5 MJ/mol of $NO_x$) [11]. In their studies, the concentration of $NO_x$ decreased significantly to ~5000

ppm with the increase in the gas flow rate from 0.5 to 1 L/min [11]. In contrast, RGA provides an effective solution to obtain a reasonable treatment capacity and a relatively low energy cost simultaneously, as shown in Figure 3.

### *3.2 Effect of oxygen concentration*

The $O_2$ concentration affects the production of $NO_x$ and energy consumption at different gas flow rates, as presented in Figure 6(a) and (b). At a gas flow rate of 4 L/min, the highest $NO_x$ concentration of ~15500 ppm is reached at an $O_2$ concentration of 30 vol.%, while the maximum $NO_x$ concentration is achieved at an $O_2$ concentration of ~40 vol.% at a higher gas flow rate (6 L/min and 8 L/min). Previous works reported that the optimal oxygen concentration in the gas mixture for the plasma production of $NO_x$ was in the range of 20 vol.% - 50 vol.% [11, 18, 29], which corroborates our results obtained with the RGA reactor. Increasing the $O_2$ concentration produces more reactive oxygen species due to the increased SEI at a higher $O_2$ concentration, thus enhancing the oxidation of nitrogen species in the plasma synthesis of $NO_x$. However, increasing the oxygen concentration to >50 vol.% reduced the $NO_x$ concentration, which can be attributed to the decrease of $N_2$ species involved in the reaction although more oxygen species are formed. Additionally, the discharge becomes unstable at a high $O_2$ concentration (>50 vol.%)

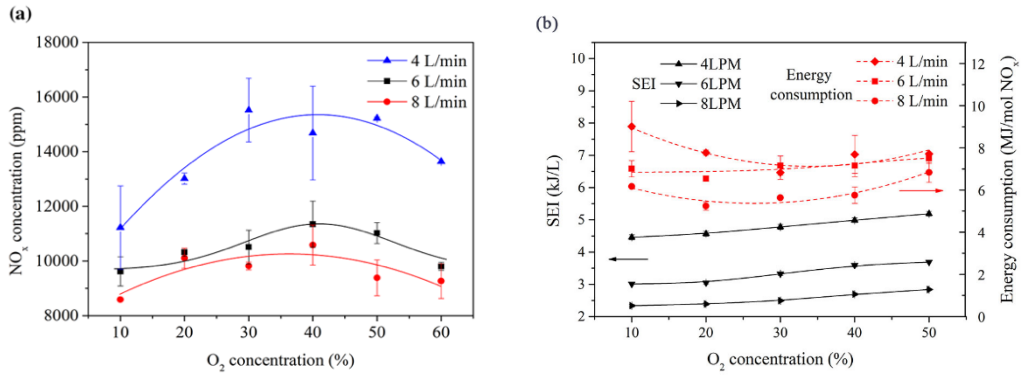


**Figure 6. The effect of $O_2$ concentration on (a) $NO_x$ concentration; (b) SEI and energy consumption (applied voltage of 10 kV).**

The influence of $O_2$ concentration on the discharge characteristics was evaluated through the analysis of the electrical signals and high-speed photography (Figure 7). In Figure 7 (a), the arc voltage and current signals show a sawtooth shape with an average value of 1.26 kV and 215 mA, respectively, suggesting the formation of a typical 'restrike' mode in the RGA discharge. In this mode, the intense and irregular fluctuations of the arc voltage are generally observed, while the electric arc was hopping over the electrodes, as shown in Figure 7(e) and (f). However, when the $O_2$ concentration reached 40 vol.%, the electrical signals were changed completely with the average arc voltage increased to 1.6 kV and the average current decreased to 210 mA. The RGA discharge then exhibits a combined 'restrike' and 'takeover' mode, with a longer rotating period, as shown in Figure 7(b)[30]. Compared to the RGA at an $O_2$ concentration of 20 vol.%, the arcs formed at an $O_2$ concentration of 40 vol.% appear blurred and fill the main zone of the reactor. Most of the arcs cannot be fully developed

before being replaced by the next arc. A smooth dazzling plasma disc with yellow clusters of the discharge was gradually formed in the RGA reactor as the $O_2$ concentration increased from 20 vol.% to 40 vol.%. In this study, we found that further increasing the $O_2$ concentration enhanced the discharge instabilities.

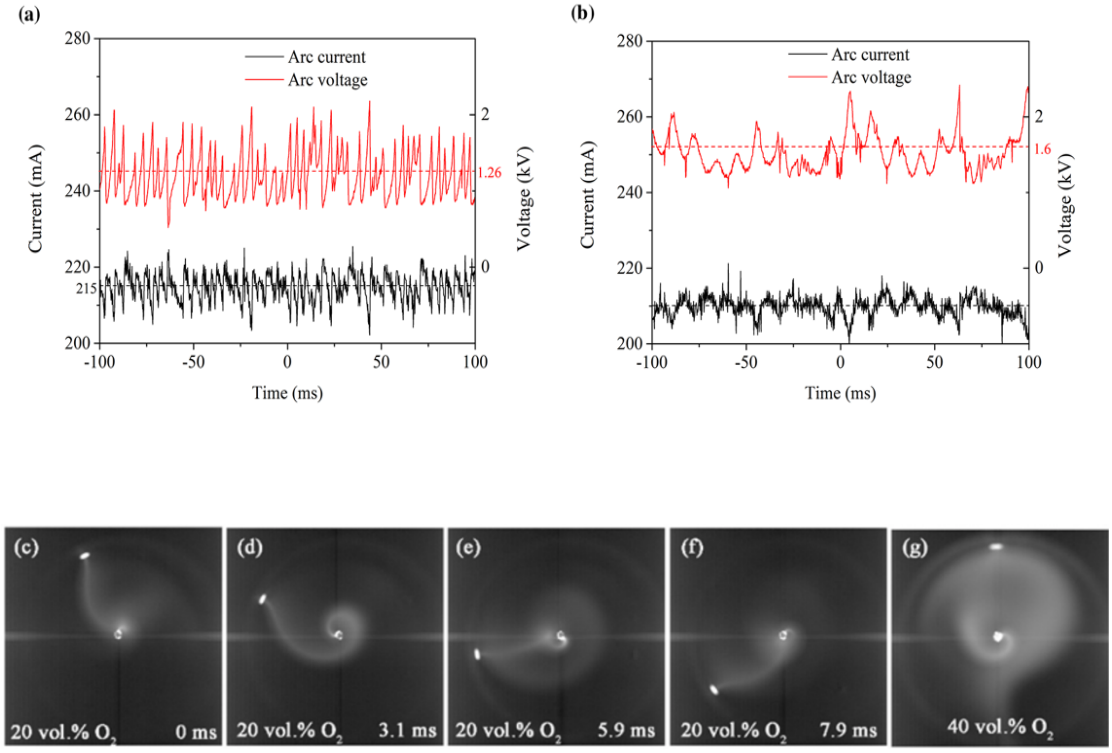


**Figure 7. Electrical signals of RGA at an $O_2$ concentration of (a) 20 vol.%; (b) 40 vol.%; (c)-(g) Dynamic characteristics of RGA captured by high-speed camera. (applied voltage of 10 kV and gas flow rate of 4 L/min)**

As increasing the $O_2$ concentration only slightly increases the SEI, the energy consumption approaches its lowest value when the $O_2$ concentration ranges between 20 vol.% and 40 vol.%. In this study, the optimal $O_2$ concentration is 20~30 vol.% to achieve the highest $NO_x$ concentration and lowest energy consumption simultaneously at a gas flow rate of 8 L/min and an applied voltage of 10 kV. The predicted values from

the ANN model are reasonably well in agreement with the experimental results in Figure 8. The model shows that increasing the $O_2$ concentration from 20 vol.% to 60 vol.% increases the energy consumption by ~50% and decreases the $NO_x$ concentration by 20%.

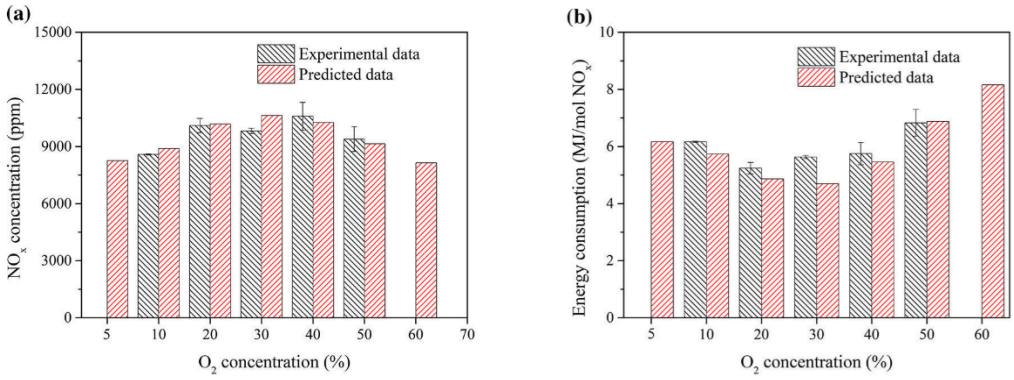


**Figure 8. Comparison of experimental and predicted data in terms of (a) $NO_x$ concentration; (b) energy consumption (gas flow rate of 8 L/min and applied voltage of 10 kV)**

### *3.3 Effect of applied voltage*

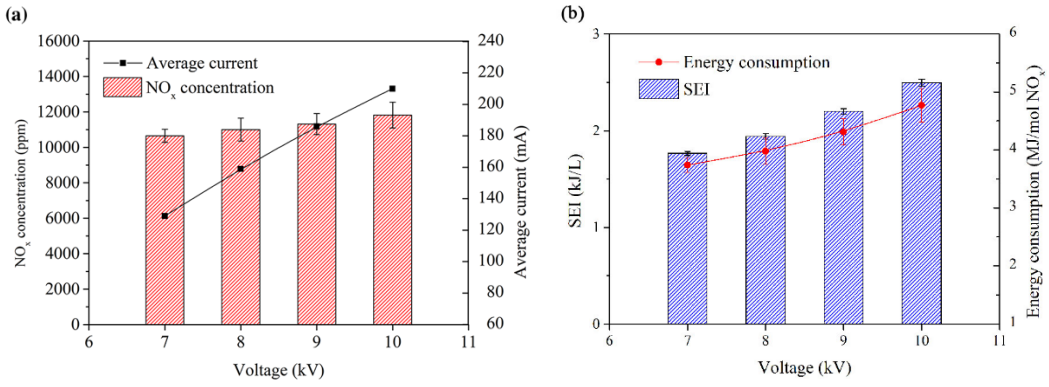

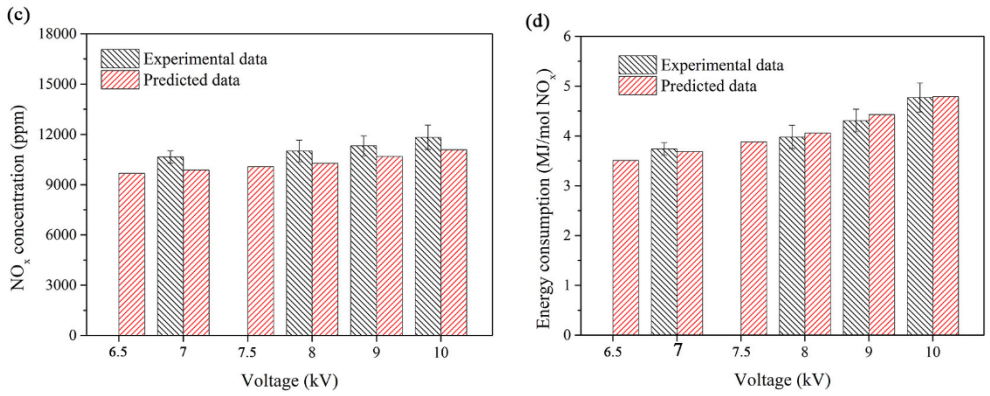


**Figure 9. The effect of applied voltage on (a) $NO_x$ concentration; (b) SEI and energy consumption. Comparison of experimental and predicted data in terms of (c) $NO_x$ concentration; (d) energy consumption (gas flow rate of 8 L/min and $O_2$ concentration of 20 vol.%)**

Figure 9 (a) shows increasing the applied voltage from 7 kV to 10 kV slightly increases the $NO_x$ concentration by 11% due to the increase of SEI. However, compared to the production of $NO_x$ ($NO_x$ concentration), the SEI is increased more significantly when rising the applied voltage. Thus, the energy consumption for $NO_x$ synthesis also increases with the increase of the applied voltage. As shown in Figure 9(b), the lowest energy consumption of 3.37 MJ/mol is achieved at 7 kV.

Figure 9 (c) and (d) show that both the simulated $NO_x$ concentration and the energy consumption are in good agreement with the experimental data. Lower energy consumption can be anticipated when further decreasing the applied voltage, as predicted by the ANN model. The applied voltage is directly linked to the energy input for the chemical reactions and the formation of reactive species and energetic electrons, thus affects the plasma chemistry in the plasma synthesis of $NO_x$, including the

enhanced electron-impact collisions (R1-R6) to facilitate the generation of N atoms, O atoms and excited $N_2$ molecules [31, 32]:

$$e + N_2 \rightarrow e + N_2(v) \quad \text{(R1)}$$

$$e + N_2 \rightarrow e + N_2(A), N_2(B), N_2(C) \quad \text{(R2)}$$

$$e + N_2 \rightarrow e + N + N \quad \text{(R3)}$$

$$e + N_2 \rightarrow e + N_2(C) \quad \text{(R4)}$$

$$e + O_2 \rightarrow e + O + O \quad \text{(R5)}$$

$$e + O \rightarrow e + O(^1S) \quad \text{(R6)}$$

Previous work also reported the dependence of the electron excitation temperature on the applied voltage in an RGA plasma [33]. On the other side, increasing the applied voltage significantly enhances the dynamic stability of the RGA discharge. We found that the arc cannot remain stable for a long period at a low applied voltage. Hence, it is not recommended to lower the applied voltage to reduce the energy consumption considering the stability of the RGA discharge. The lowest energy consumption predicted by our ANN model could be achieved at an applied voltage of 6.5 kV. Further work will attempt to enhance the stability of the RGA at lower applied voltages by optimizing the reactor and/or power design.

### *3.4 Correlation between SEI and $NO_x$ concentration*

In this study, the SEI is affected by the applied voltage, the flow rate and the $O_2$ concentration, and is intimately correlated with the $NO_x$ concentration. Figure 10 indicates a quasi-linear and positive correlation between the SEI and the $NO_x$

concentration. Clearly, increasing the SEI enhances the production of $NO_x$ using either air or a mixture of $N_2$ and $O_2$.

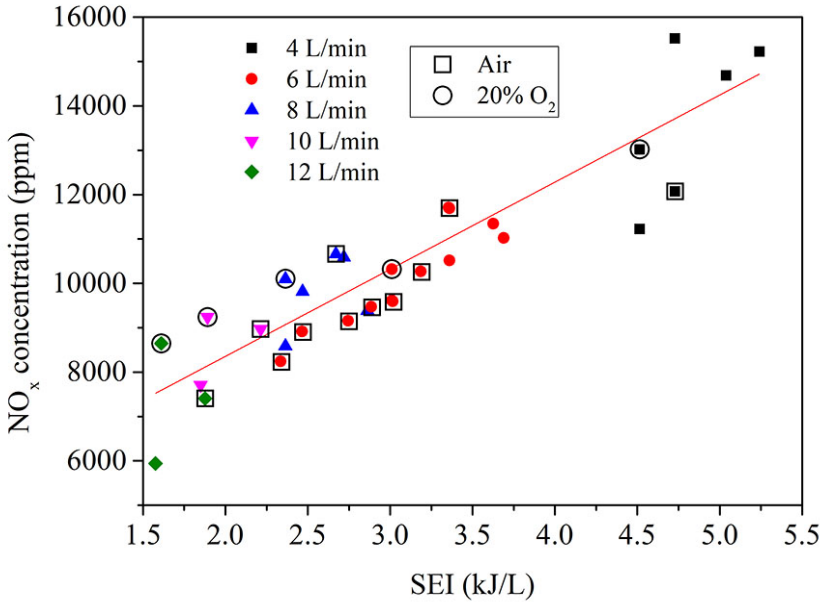


**Figure 10. Correlation between SEI and $NO_x$ concentration**

In this work, the lowest energy consumption for $NO_x$ production in the $N_2/O_2$ discharge and air discharge is 4.2 MJ/mol and 5.5 MJ/mol, respectively. In addition, our RGA process shows a balanced low energy consumption and large processing capacity (4-12 L/min) compared to other types of non-thermal plasmas (Table 1). The summarized results in Table 1 show that GA especially RGA has great potential to lower the energy consumption of $NO_x$ production for sustainable nitrogen fixation. Vervloessem et al. reported an energy consumption of 3.6 MJ/mol in the synthesis of $NO_x$ from a mixture of $N_2$ and $O_2$ using a GA plasma [34]. Jardali et al. investigated the $NO_x$ production using a RGA reactor operated in two arc modes (rotating and stable modes). The $NO_x$ concentrations up to 5.5% were achieved with the lowest energy

consumption of 2.5 MJ/mol when the arc was operated in a stable mode [39].

**Table 1. Comparison of the performance for $NO_x$ synthesis using different atmospheric pressure NTPs**

| Plasma | Gas | Gas flow rate (L/min) | $O_2$ Concentration (Vol.%) | Power (W) | $NO_x$ concentration (ppm) | Optimal energy consumption (MJ/mol $NO_x$) | Reference |
|---|---|---|---|---|---|---|---|
| Spark plasma | Air | Batch (15 min) | 21 | - | - | 20.3 | [35] |
| Spark plasma | Air | Batch (10 min) | 21 | 4.45-26.7 | 2000-6300 | 40 | [36] |
| Spark plasma | - | Batch | - | 4-5 | - | 5.2 | [18] |
| Glow discharge | Air | 2 | 21 | - | - | 7 | [18] |
| Propeller arc | Air | 3 | 1.6-98.5 | 0~133 | 0~4462 | 3.5 | [18] |
| | $N_2/O_2$ mixture | | | | | | |

| | | | | | | | |
|---|---|---|---|---|---|---|---|
| DBD | $N_2/O_2$ mixture | Batch (6-7 min) | 20-100 | - | 6000 | 20 | [37] |
| GA | $N_2/O_2$ mixture | 0.5-1 | 20-70 | 12-40 | 2000-14000 | 4.8 | [37] |
| Plasma jet | Air | 8.8-66 | 21 | 65-165 | 1000-3500 | 3.4 | [27] |
| Plasma jet | Air | 0.25-8 | 21 | 0.6-27 | 100-1000 | 8.6 | [26] |
| Spark plasma | $N_2/O_2$ mixture | 1.3-2.6 | 20 | 0-6 | 100-600 | 8.6 | [38] |
| GA | $N_2/O_2$ mixture | 10 | 10-90 | 369 | 15000 | 3.6 | [34] |
| RGA | $N_2/O_2$ mixture | 2 | 50% | 180-200 | 55000 | 2.5 | [39] |
| RGA | $N_2/O_2$ mixture | 4-12 | 10-50 | 300-382 | 5900-15500 | 4.2 | This work |
| RGA | Air | 4-12 | 21 | 315-375 | 7400-12000 | 5.5 | This work |

### *3.5 Coupling effect and importance of different process parameters*

The effect of different operating parameters and their interactions on the $NO_x$ concentration and energy consumption of the plasma nitrogen fixation process was investigated using the ANN model and the three-dimensional surface plots of the results are presented in Figures S1-6. Figures S1 and S2 show the combined effect of the gas flow rate and $O_2$ concentration on the $NO_x$ concentration and energy consumption at different applied voltages. The results from the ANN model indicate that the highest $NO_x$ concentration and the lowest energy consumption can be achieved at a gas flow rate of 2 L/min and an $O_2$ concentration of 40 vol.% with the applied voltage of 10 kV. The change in the applied voltage does not have a significant effect on the reaction performance, as only a slight variation of the three-dimensional surface is observed when changing the applied voltage. The coupled effect of the applied voltage and $O_2$ concentration on the nitrogen fixation process at different gas flow rates is presented in Figures S3 and S4. Regardless of the applied voltage, we find that the $NO_x$ concentration is considerably affected by varying the $O_2$ concentration, while the three-dimensional surface reaches its valley of minimal energy consumption at an $O_2$ concentration of 20 vol.%-30 vol.%. As shown in Figures S5 and S6, decreasing the gas flow rate and increasing the applied voltage substantially increases the production of $NO_x$ but also increases the energy consumption simultaneously. Predicted by our model, the highest $NO_x$ concentration of ~16000 ppm can be reached at a gas flow rate of 2 L/min, with the lowest energy consumption of ~2.8 MJ/mol for $NO_x$ production. Figure S7 shows the effect of gas flow rate and applied voltage on the plasma synthesis of $NO_x$ from the air. The experimental results fit well with the grids produced by the ANN

model. The optimal energy consumption can be obtained when the gas flow rate varies between 8 L/min and 12 L/min.

Figure 11 presents the relative importance of different process parameters on the plasma synthesis of $NO_x$ in this study (see explanation in section 2.2). The gas flow rate is found to be the most critical parameter affecting the $NO_x$ concentration with a relative importance of 58.7 %, while the $O_2$ concentration is the most important process parameter to determine the energy consumption for $NO_x$ production with a weight of ~48.5 %. Among the three process parameters, applied voltage is the least important parameter affecting the production of $NO_x$ in this process. The relative importance of the process parameters on the $NO_x$ concentration decreases as follows: gas flow rate > $O_2$ concentration > applied voltage, while the relative importance of the process parameters on the energy consumption follows the order: $O_2$ concentration > flow rate > applied voltage.

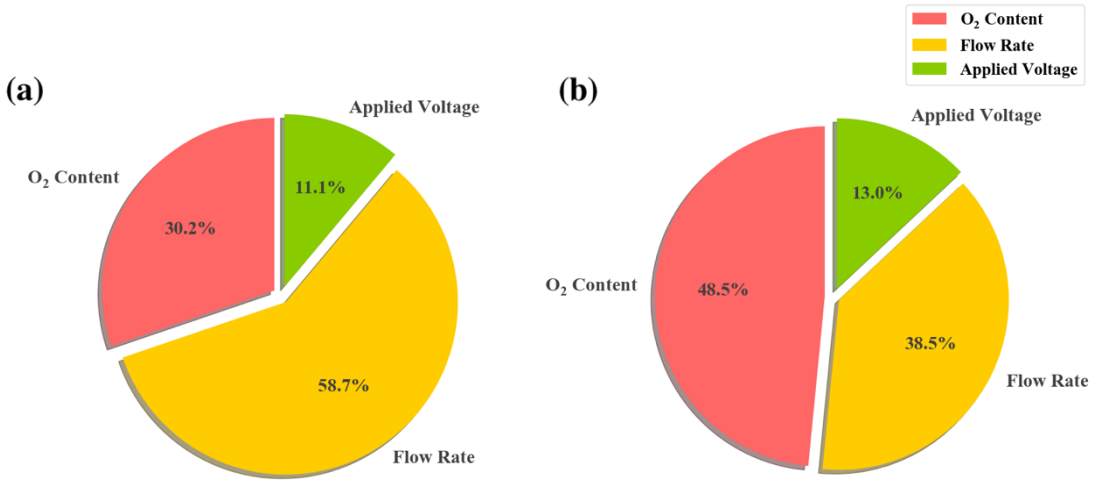


**Figure 11. Relative importance (%) of different process parameters on (a) $NO_x$ concentration; (b) energy consumption.**

### 3.6 Roles of reactive species in nitrogen fixation via air oxidation by RGA plasma

The highly efficient $NO_x$ production using the RGA discharge is a result of the reactive plasma chemistry, which generates the energetic electrons and reactive species for chemical reactions. Herein, the emission spectrum of the $N_2/O_2$ RGA shows molecular bands including $N_2$ second positive systems (SPS), $N_2^+$ first negative system (FNS), NO (A-X) and $O_2$ (B-X), while OH molecules bands are also visible in the emission spectrum of the air RGA (Table S2). Previous plasma modeling studies revealed that the vibrationally excited $N_2$ molecules could significantly contribute to the production of $NO_x$ in GA plasmas as the typical reduced electric field (E/N, where E is the electric field and N is the concentration of neutral particles) of GA is in the range of 5-100 Td [15, 20, 31]. This range of the reduced electric field could also apply to the RGA plasma in this study. For example, Jardali et al. used the reduced electric field of 5-30 Td in the modeling of $NO_x$ production in an RGA reactor [40]. Recent works reported that vibrational excitation can enhance the generation of $NO_x$ through the conventional Zeldovich mechanism[20, 34, 39].

$$N_2(v) + O \rightarrow NO + N \quad \text{(R7)}$$

$$O_2(v) + N \rightarrow NO + O \quad \text{(R8)}$$

$NO_2$ can be formed through the further oxidation of NO by O atoms[20, 40].

$$NO + O \rightarrow NO_2 \quad \text{(R9)}$$

## 4.Conclusion:

In this work, we demonstrate that the RGA plasma can synthesize $NO_x$ from a

mixture of $N_2$ and $O_2$ or air with relatively low energy consumption and high processing capacity. The lowest energy consumption for $NO_x$ production (4.2 MJ/mol) is achieved at an applied voltage of 10 kV, a gas flow rate of 12 L/min and an $O_2$ concentration of 20 vol.%. The results from the ANN model agree well with the experimental data. The relative importance of the process parameters on the $NO_x$ concentration follows the order: gas flow rate > $O_2$ concentration > applied voltage, while the relative importance of the process parameters on the energy consumption of $NO_x$ formation decreases in the order: $O_2$ concentration > gas flow rate > applied voltage. Higher gas flow rates result in a decrease of the $NO_x$ concentration and energy cost. On the other hand, increasing the applied voltage slightly enhances the reaction performance in terms of $NO_x$ concentration, but it is accompanied by the increased SEI and energy cost. The optimal $O_2$ concentration for $NO_x$ synthesis is in the range of 20 vol.% to 40 vol.%, the results show that air can be directly converted to $NO_x$ using the RGA reactor. This work has shown that RGA plasmas have great potential to be developed as a small-scale and on-demand process powered by renewable energy sources (e.g., wind and solar power) for nitrogen fixation directly from the air, thus contributing to green industrial development. Nevertheless, more works are still required to further decrease the energy cost for $NO_x$ production whilst increase the yield of $NO_x$. For instance, combining the RGA system with suitable catalysts has the potential to further enhance the reaction performance.

**Acknowledgements:**

Stephanie Mathieu and Xin Tu acknowledge the European Union (EU) and Horizon 2020 funding awarded under the Marie Sklodowska-Curie Action to the EUROPAH Consortium (grant number 722346). This study is supported by the Young Scientists Fund of the National Natural Science Foundation of China (51806193), National Natural Science Foundation of China (51976191), and Innovative Research Groups of the National Natural Science Foundation of China (51621005).

## Reference:

[1] J.G. Chen, R.M. Crooks, L.C. Seefeldt, K.L. Bren, R.M. Bullock, M.Y. Darensbourg, P.L. Holland, B. Hoffman, M.J. Janik, A.K. Jones, M.G. Kanatzidis, P. King, K.M. Lancaster, S.V. Lymar, P. Pfromm, W.F. Schneider, R.R. Schrock, Beyond fossil fuel-driven nitrogen transformations, Science, 360 (2018).
[2] N. Cherkasov, A.O. Ibhadon, P. Fitzpatrick, A review of the existing and alternative methods for greener nitrogen fixation, Chemical Engineering and Processing: Process Intensification, 90 (2015) 24-33.
[3] Y. Tanabe, Y. Nishibayashi, Developing more sustainable processes for ammonia synthesis, Coordination Chemistry Reviews, 257 (2013) 2551-2564.
[4] R.R. Schrock, Reduction of dinitrogen, Proceedings of the National Academy of Sciences, 103 (2006) 17087.
[5] A. Bogaerts, E.C. Neyts, Plasma Technology: An Emerging Technology for Energy Storage, ACS Energy Letters, 3 (2018) 1013-1027.
[6] A. Bogaerts, X. Tu, J. Whitehead, G. Centi, L. Lefferts, O. Guaitella, F. Jury, H.-H. Kim, A. Murphy, W. Schneider, T. Nozaki, J. Hicks, A. Rousseau, F. Thevenet, A. Khacef, M. Carreon, The 2020 plasma catalysis roadmap, Journal of Physics D: Applied Physics, 53 (2020) 443001.
[7] X. Hu, X. Zhu, X. Wu, Y. Cai, X. Tu, Plasma-enhanced NH3 synthesis over activated carbon-based catalysts: Effect of active metal phase, Plasma Processes and Polymers, 17 (2020) 2000072.
[8] H.-H. Kim, Y. Teramoto, A. Ogata, H. Takagi, T. Nanba, Atmospheric-pressure nonthermal plasma synthesis of ammonia over ruthenium catalysts, Plasma Processes and Polymers, 14 (2017) 1600157.
[9] K.H.R. Rouwenhorst, Y. Engelmann, K. van ‘t Veer, R.S. Postma, A. Bogaerts, L. Lefferts, Plasma-driven catalysis: green ammonia synthesis with intermittent electricity, Green Chemistry, 22 (2020) 6258-6287.
[10] Y. Wang, M. Craven, X. Yu, J. Ding, P. Bryant, J. Huang, X. Tu, Plasma-Enhanced Catalytic Synthesis of Ammonia over a Ni/Al2O3 Catalyst at Near-Room Temperature: Insights into the Importance of the Catalyst Surface on the Reaction Mechanism, ACS Catalysis, 9 (2019) 10780-10793.
[11] B.S. Patil, F.J.J. Peeters, G.J. van Rooij, J.A. Medrano, F. Gallucci, J. Lang, Q. Wang, V. Hessel, Plasma assisted nitrogen oxide production from air: Using pulsed powered gliding arc reactor for a containerized plant, AIChE Journal, 64 (2018) 526-537.

[12] H.S. Eyde, THE MANUFACTURE OF NITRATES FROM THE ATMOSPHERE BY THE ELECTRIC ARC—BIRKELAND-EYDE PROCESS, Journal of the Royal Society of Arts, 57 (1909) 568-576.
[13] P. Chawdhury, Y. Wang, D. Ray, S. Mathieu, N. Wang, J. Harding, F. Bin, X. Tu, S. Challapalli, A promising plasma-catalytic approach towards single-step methane conversion to oxygenates at room temperature, Applied Catalysis B: Environmental, 284 (2020) 119735.
[14] A. George, B. Shen, M. Craven, Y. Wang, D. Kang, W. Chunfei, X. Tu, A Review of Non-Thermal Plasma Technology: A novel solution for CO2 conversion and utilization, Renewable and Sustainable Energy Reviews, 135 (2021) 109702.
[15] V.D. Rusanov, A.A. Fridman, G.V. Sholin, The physics of a chemically active plasma with nonequilibrium vibrational excitation of molecules, Soviet Physics Uspekhi, 24 (1981) 447-474.
[16] R.F. Service, Renewable bonds, Science, 365 (2019) 1236.
[17] D.B. Graves, L.B. Bakken, M.B. Jensen, R. Ingels, Plasma Activated Organic Fertilizer, Plasma Chemistry and Plasma Processing, 39 (2018) 1-19.
[18] X. Pei, D. Gidon, Y.-J. Yang, Z. Xiong, D.B. Graves, Reducing energy cost of NOx production in air plasmas, Chemical Engineering Journal, 362 (2019) 217-228.
[19] J. Yang, T. Li, C. Zhong, X. Guan, C. Hu, Nitrogen Fixation in Water Using Air Phase Gliding Arc Plasma, Journal of The Electrochemical Society, 163 (2016) E288-E292.
[20] W. Wang, B. Patil, S. Heijkers, V. Hessel, A. Bogaerts, Nitrogen Fixation by Gliding Arc Plasma: Better Insight by Chemical Kinetics Modelling, ChemSusChem, 10 (2017) 2145-2157.
[21] T. Chang, J.Q. Lu, Z.X. Shen, Y. Huang, D. Lu, X. Wang, J.J. Cao, R. Morent, Simulation and optimization of the post plasma-catalytic system for toluene degradation by a hybrid ANN and NSGA-II method, Appl. Catal. B-Environ., 244 (2019) 107-119.
[22] X.B. Zhu, S.Y. Liu, Y.X. Cai, X. Gao, J.S. Zhou, C.H. Zheng, X. Tu, Post-plasma catalytic removal of methanol over Mn-Ce catalysts in an atmospheric dielectric barrier discharge, Appl. Catal. B-Environ., 183 (2016) 124-132.
[23] Y. Wang, Z. Liao, S. Mathieu, F. Bin, X. Tu, Prediction and evaluation of plasma arc reforming of naphthalene using a hybrid machine learning model, Journal of Hazardous Materials, 404 (2021) 123965.
[24] S.Y. Liu, D.H. Mei, Z. Shen, X. Tu, Nonoxidative Conversion of Methane in a Dielectric Barrier Discharge Reactor: Prediction of Reaction Performance Based on Neural Network Model, The Journal of Physical Chemistry C, 118 (2014) 10686-10693.
[25] D.H. Lee, K.T. Kim, M.S. Cha, Y.H. Song, Optimization scheme of a rotating gliding arc reactor for partial oxidation of methane, Proceedings of the Combustion Institute, 31 (2007) 3343-3351.
[26] X. Hao, A.M. Mattson, C.M. Edelblute, M.A. Malik, L.C. Heller, J.F. Kolb, Nitric Oxide Generation with an Air Operated Non-Thermal Plasma Jet and Associated Microbial Inactivation Mechanisms, Plasma Processes and Polymers, 11 (2014) 1044-1056.
[27] Y.D. Korolev, O.B. Frants, N.V. Landl, A.I. Suslov, Low-Current Plasmatron as a Source of Nitrogen Oxide Molecules, IEEE Transactions on Plasma Science, 40 (2012) 2837-2842.
[28] A.V. Pekshev, A.B. Shekhter, A.B. Vagapov, N.A. Sharapov, A.F. Vanin, Study of plasma-chemical NO-containing gas flow for treatment of wounds and inflammatory processes, Nitric Oxide, 73 (2018) 74-80.
[29] B.S. Patil, N. Cherkasov, J. Lang, A.O. Ibhadon, V. Hessel, Q. Wang, Low temperature plasma-catalytic NO x synthesis in a packed DBD reactor: Effect of support materials and supported active metal oxides, Applied Catalysis B: Environmental, 194 (2016) 123-133.

[30] H. Zhang, F. Zhu, X. Tu, Z. Bo, K. Cen, X. Li, Characteristics of Atmospheric Pressure Rotating Gliding Arc Plasmas, Plasma Science and Technology, 18 (2016) 473-477.
[31] L.V. Gatilova, K. Allegraud, J. Guillon, Y.Z. Ionikh, G. Cartry, J. Röpcke, A. Rousseau, NO formation mechanisms studied by infrared laser absorption in a single low-pressure plasma pulse, Plasma Sources Science and Technology, 16 (2007) S107-S114.
[32] R. Brandenburg, V.A. Maiorov, Y.B. Golubovskii, H.E. Wagner, J. Behnke, J.F. Behnke, Diffuse barrier discharges in nitrogen with small admixtures of oxygen: discharge mechanism and transition to the filamentary regime, Journal of Physics D: Applied Physics, 38 (2005) 2187-2197.
[33] A. Wu, H. Zhang, X. Li, S. Lu, C. Ming Du, J. Hua Yan, Spectroscopic Diagnostics of Rotating Gliding Arc Plasma Codriven by a Magnetic Field and Tangential Flow, 2014.
[34] E. Vervloessem, M. Aghaei, F. Jardali, N. Hafezkhiabani, A. Bogaerts, Plasma-Based N2 Fixation into NOx: Insights from Modeling toward Optimum Yields and Energy Costs in a Gliding Arc Plasmatron, ACS Sustainable Chemistry & Engineering, 8 (2020) 9711-9720.
[35] N. Rehbein, V. Cooray, NOx production in spark and corona discharges, Journal of Electrostatics, 51-52 (2001) 333-339.
[36] M.J. Pavlovich, T. Ono, C. Galleher, B. Curtis, D.S. Clark, Z. Machala, D.B. Graves, Air spark-like plasma source for antimicrobial NOxgeneration, Journal of Physics D: Applied Physics, 47 (2014).
[37] B. Patil, Plasma (Catalyst) Assisted Nitrogen Fixation: Reactor Development for Nitric Oxide and Ammonia Production, 2017.
[38] M. Janda, V. Martišovitš, K. Hensel, Z. Machala, Generation of Antimicrobial NOx by Atmospheric Air Transient Spark Discharge, Plasma Chemistry and Plasma Processing, 36 (2016) 767-781.
[39] F. Jardali, S. Van Alphen, J. Creel, H. Ahmadi Eshtehardi, M. Axelsson, R. Ingels, R. Snyders, A. Bogaerts, NOx production in a rotating gliding arc plasma: potential avenue for sustainable nitrogen fixation, Green Chemistry, (2021).
[40] W. Gaens, A. Bogaerts, Kinetic modelling for an atmospheric pressure argon plasma jet in humid air, JOURNAL OF PHYSICS D-APPLIED PHYSICS, 46 (2013).